Journal of
MATERIALS RESEARCH

Synthesis of pure amorphous Fe_2O_3

X. Cao
Department of Chemistry, Bar-Ilan University, Ramat-Gan, Israel, 52900

R. Prozorov
Department of Physics, Bar-Ilan University, Ramat-Gan, Israel, 52900

Yu. Koltypin and G. Kataby
Department of Chemistry, Bar-Ilan University, Ramat-Gan, Israel, 52900

I. Felner
Racah Institute of Physics, Hebrew University, Jerusalem, Israel

A. Gedanken
Department of Chemistry, Bar-Ilan University, Ramat-Gan, Israel, 52900

(Received 1 April 1996; accepted 26 August 1996)

A method for the preparation of pure amorphous Fe_2O_3 powder with particle size of 25 nm is reported in this article. Pure amorphous Fe_2O_3 can be simply synthesized by the sonication of neat $Fe(CO)_5$ or its solution in decalin under an air atmosphere. The Fe_2O_3 nanoparticles are converted to crystalline Fe_3O_4 nanoparticles when heated to 420 °C under vacuum or when heated to the same temperature under a nitrogen atmosphere. The crystalline Fe_3O_4 nanoparticles were characterized by x-ray diffraction and Mössbauer spectroscopy. The Fe_2O_3 amorphous nanoparticles were examined by Transmission Electron Micrography (TEM), Differential Scanning Calorimetry (DSC), Thermogravimetric Analysis (TGA), and Quantum Design SQUID magnetization measurements. The magnetization of pure amorphous Fe_2O_3 at room temperature is very low (<1.5 emu/g) and it crystallizes at 268 °C.

I. INTRODUCTION

Amorphous metal oxides have many important applications, including that in the fields of solar-energy transformation, magnetic storage media, electronics, and catalysis.[1–5] Amorphous metal oxides can be prepared by rapidly quenching the molten mixture of metal oxides and a glass former, such as P_2O_5, V_2O_5, Bi_2O_3, SiO_2, and CaO,[1,6–8] or by thermal decomposition of some easily decomposed metal compounds.[4,9] Amorphous metal oxide thin films on a substrate can be prepared by means of ion beam sputtering, electron beam evaporation, and thermal evaporation.[10] So far, only a few amorphous metal oxides, such as Cr_2O_3, V_2O_5, MnO_2, and PbO_2 powders, have been prepared by means of thermal decomposition,[4,9] but it is difficult to control their purities. Other amorphous metal oxides are usually in the form of hydrous oxides.[5,11] The cooling rates that are generally required for the preparation of amorphous metals are 10^5–10^7 K/s. Since the thermal conductivities of metal oxides are usually much lower than those of the metals, faster cooling rates are needed to prepare amorphous metal oxides. This is the reason that glass formers, whose purpose is preventing crystallization, are added if the quenching method is applied. No pure amorphous iron oxide has ever been reported as being successfully prepared. Suslick and his co-workers have reported the preparation of amorphous iron,[12] amorphous cobalt, and amorphous Fe/Co alloy,[13] as well as amorphous molybdenum carbide,[14] all as powders having nanometer size particles. These amorphous compounds were prepared by sonochemical means. The cooling rates obtained during the cavitational collapse, which is the most important event in the sonochemical process, are estimated to be greater than 2×10^9 K/s and may be as large as 10^{13} K/s. The magnetic properties of the amorphous iron nanoparticles were also studied by Suslick's group.[15] Following Suslick we have recently been able to demonstrate that the size of the amorphous iron nanoparticles can be controlled.[16] We have also sonicated $Ni(CO)_4$ and obtained amorphous Ni.[17] In this paper we report on our success in preparing amorphous Fe_2O_3 using sonochemical methods.

II. EXPERIMENTAL

The preparation of pure amorphous Fe_2O_3 is similar to that of amorphous iron; namely, pure $Fe(CO)_5$ (Aldrich), or its solution in decalin (Fluka), is irradiated with a high intensity ultrasonic horn (Ti-horn, 20 kHz) under 1.5 atm of air at 0 °C for 3 h. The product is washed thoroughly with dry pentane. This method is

found to yield exclusively Fe_2O_3, while the other two methods, using O_2 instead of air, or washing the product in an inert glovebox, leave unreacted amorphous iron as a product. The best method is therefore the one in which the entire preparative procedure is carried out under normal air atmosphere.

III. RESULTS

Elemental analysis by EDX (Energy Dispersive X-ray Spectroscopy) shows that the resulting black powder contains only the elements Fe, O, and a trace of C (estimated $<2\%$). Conventional elemental analysis gave a molar ratio of O:Fe ranging from 1.5:1 to 2:1. The higher ratio is due to the strong adsorption of oxygen on the resulting nanoparticles. To determine whether any Fe^{+2} ions exist in the product, we have performed the α, α'-phenanthroline spot test.[18] This test gave a negative result for the amorphous powder which is the sonication product, while positive results are obtained for commercial Fe_3O_4 as well as FeO. In Fig. 1 we present the XRD patterns of (i) amorphous Fe_2O_3, (ii) crystalline Fe_3O_4 which is obtained when the amorphous Fe_2O_3 is heated in nitrogen to 420 °C for 1 h (the same pattern is obtained when the amorphous Fe_2O_3 is heated to 420 °C under vacuum), and (iii) crystalline $\gamma-Fe_2O_3$ which is obtained when the amorphous sample is heated to 420 °C in air. We have also added to this figure the pattern measured for commercial crystalline Fe_3O_4. The conversion of Fe_2O_3 to Fe_3O_4 by heating the amorphous sample in nitrogen and in vacuum is to be expected, since it has been reported to occur in vacuum at 250 °C.[19] The heating in air is avoiding the conversion to Fe_3O_4 because the oxygen pressure shifts the equilibrium toward the reactants. The XRD is measured on a Model-2028 (Rigaku) diffractometer. The assignment is based on comparison to the ASTM cards.

The Mössbauer spectra (MS) is presented in Fig. 2. It was measured at 300 K using a conventional constant acceleration spectrometer. The ^{57}Fe MS was monitored with a 20 mCi $^{57}Co:Rh$ source, and the spectra were least-square fitted with one or two subspectra. Figure 2 displays the MS spectra of amorphous Fe_2O_3 and crystalline Fe_3O_4 which is obtained after heating the sonicated product to 420 °C under vacuum, and commercial crystalline $\gamma-Fe_2O_3$. For the amorphous sample, the central part of the spectrum exhibits only a broad doublet, which indicates clearly that no long-range magnetic ordering exists. The main information obtained from both visual and computer analysis is the presence

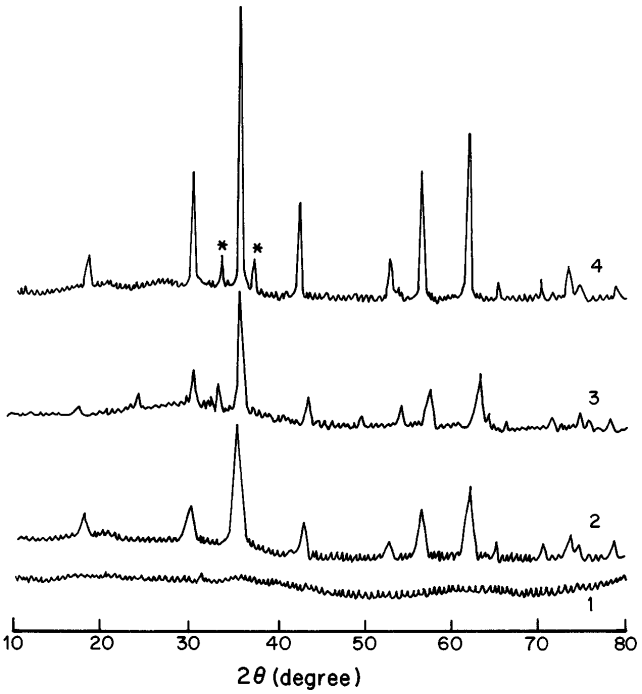

FIG. 1. XRD patterns of (1) amorphous Fe_2O_3, (2) crystalline Fe_3O_4 obtained by heating the amorphous Fe_2O_3 sample to 420 °C in nitrogen, (3) crystalline Fe_2O_3 obtained by heating the amorphous sample to 420 °C, and (4) commercial Fe_3O_4. (*) Please note that these peaks should not appear in the spectrum if the Fe_3O_4 is of high purity.

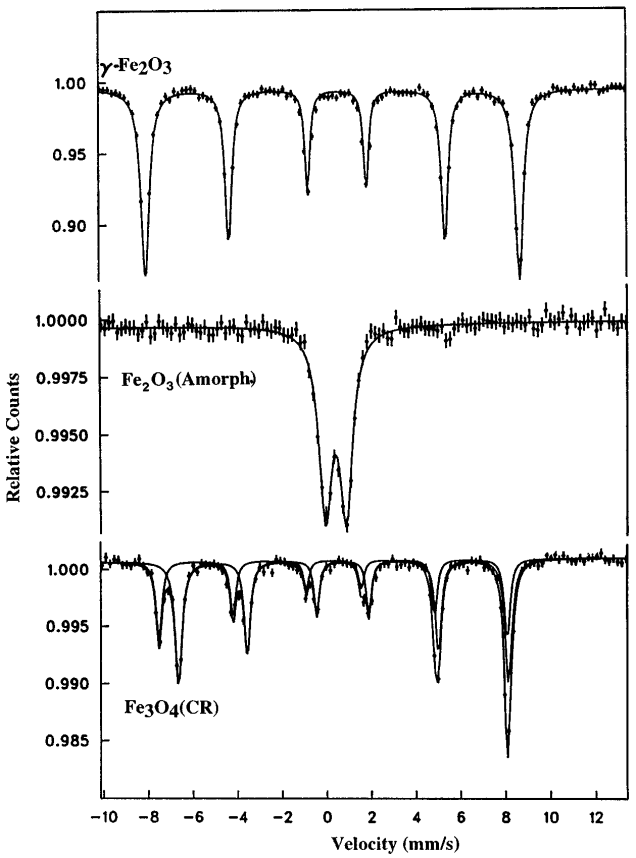

FIG. 2. Mössbauer spectra of crystalline $\gamma-Fe_2O_3$, amorphous Fe_2O_3 (amorph.), and crystalline Fe_3O_4 (CR), obtained by heating the amorphous Fe_2O_3 to 420 °C in vacuum. The spectra were measured at room temperature.

of two or three quadrupole doublets, corresponding to nonequivalent Fe sites in the amorphous material. Artificially, the doublet was fitted with one subspectra, with the following hyperfine parameters: isomer shift (IS) = 0.42(1) (relative to iron metal) and quadrupole splitting $\Delta = eqQ/2 = 0.93(1)$, and a linewidth of 70(1) mm/s.

The MS spectrum of the crystalline Fe_3O_4 reveals hyperfine magnetic splitting, which is clear evidence for long-range magnetic ordering at low temperatures. It also provides an unequivocal identification of the product obtained from the heating of the amorphous Fe_2O_3 as Fe_3O_4. The interpretation of the spectrum is based on the well-established site assignment of Fe_3O_4 (magnetite). In this structure the Fe^{+2} ions reside in the octahedral site (B site), whereas 2 Fe^{+3} ions are distributed over the tetrahedral (A site) and B sites. This spectrum is fitted with two sextets, and the hyperfine parameters are as follows. For the most intense subspectrum, whose intensity is 65% of the spectral area, which corresponds to the Fe^{+3} ions, the magnetic hyperfine field is $H_{eff} = 457(2)$ kOe, and IS = 0.70(1) mm/s. For the sextet which is attributed to Fe^{+2} $H_{eff} = 485(2)$ kOe, and IS 0.17(1) mm/s. The fast electron-transfer process (electron hopping) between the Fe ions produces a completely averaged spectrum from these ions, which do not show a quadrupole effect. The recorded data are in good agreement with well-known hyperfine parameters for Fe_3O_4.[20]

For the sake of comparison, the MS of γ–Fe_2O_3 is also shown in Fig. 2. The fit of this spectrum yields the following parameters: IS = 0.24(1) mm/s and H_{eff} = 520(1) kOe, and the effective quadrupole splitting is −0.20(1) mm/s.

Figure 3 depicts the TEM picture of amorphous Fe_2O_3 powder. There is no evidence for a crystalline formation in this powder. The amorphous Fe_2O_3 is an agglomerate of small particles with diameters of about 25 nm. Most of these particles are aggregated in a spongelike form, and therefore it is difficult to determine precisely the diameter of the individual particle. The mean size of the aggregates is about 190 ± 50 nm, as determined by means of submicron particle size analysis (COULTER Model N4).

Figure 4 displays the DSC of amorphous Fe_2O_3. The large exothermic peak at 268 °C is attributed to the crystallization of the amorphous Fe_2O_3. A similar exothermic peak is detected for the crystallization of the amorphous iron at 310 °C.[12] The heat of the transition from the amorphous state to the crystalline state is about 20 kJ/mole.

In Fig. 5 we present the TGA of amorphous Fe_2O_3, as well as two other samples of Fe_3O_4 (a commercial sample, and a second sample which is the result of heating Fe_2O_3 to 900 °C in nitrogen), measured in a magnetic field. The sharp drop in weight (or force)

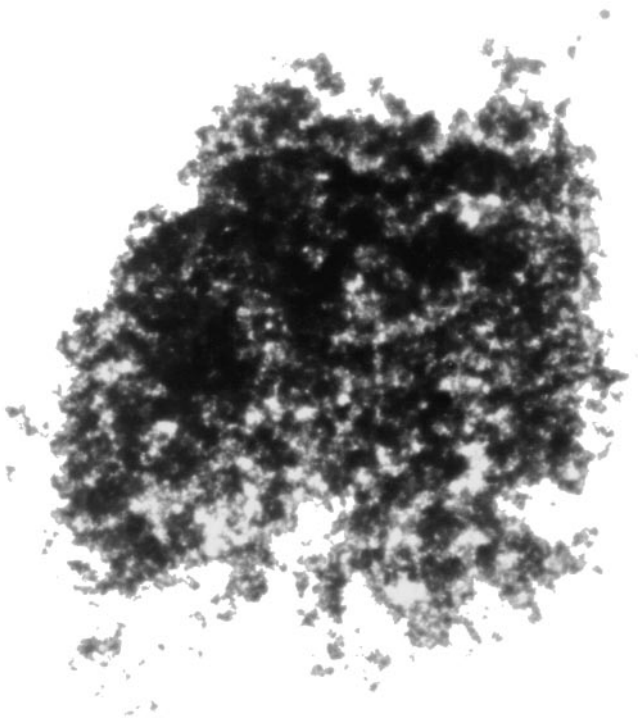

FIG. 3. A TEM picture of amorphous Fe_2O_3.

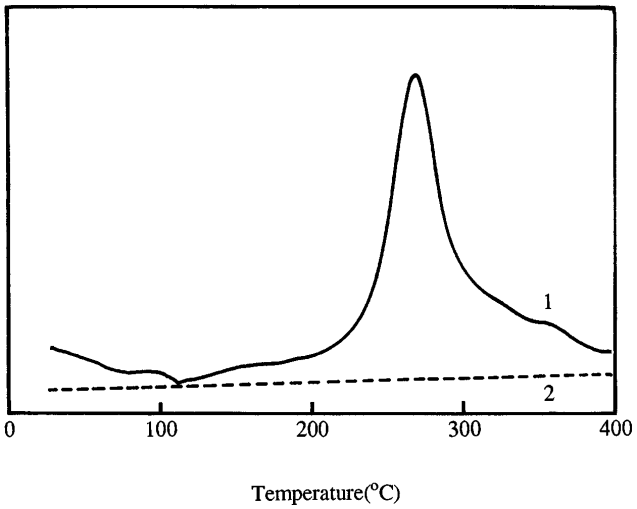

FIG. 4. DSC curves of (1) amorphous Fe_2O_3 and (2) crystalline Fe_3O_4, obtained by heating the amorphous sample to 420 °C in nitrogen. The heating rate is 10 K/min. Nitrogen of high purity is flown through the system during the measurement.

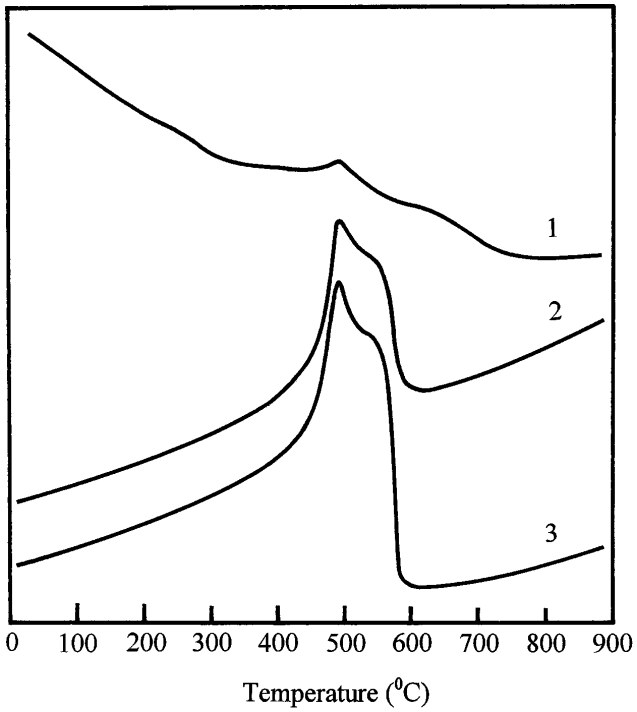

FIG. 5. TGA curves in an external magnetic field of (1) amorphous Fe_2O_3, (2) crystalline Fe_3O_4 obtained by heating the amorphous sample to 900 °C in nitrogen, and (3) commercial Fe_3O_4. The heating rate is 10 K/min, in high purity nitrogen.

at 575 °C is due to the Curie temperature of Fe_3O_4.[15] The peak observed for the Fe_3O_4 samples at 480 °C can also be detected in the amorphous Fe_2O_3 spectrum at the same temperature. This is in accordance with our findings that the Fe_2O_3 is decomposed to Fe_3O_4 in nitrogen at 420 °C (or at even lower temperatures). The TGA measurements were carried out under nitrogen, and despite a 10 K/min heating rate, the material is partly decomposed at 480 °C and reveals a peak at this temperature. The general loss of weight, which is observed in the amorphous Fe_2O_3 spectrum over a wide temperature range, is due to its conversion to Fe_3O_4.

Figure 6 presents the magnetization loop of amorphous Fe_2O_3. The magnetization of ferromagnetic materials is very sensitive to the microstructure of a particular sample. If a specimen consists of small particles, its total magnetization decreases with particle size, due to increasing dispersion on the exchange integral.[21] It finally reaches the superparamagnetic state, when each particle acts as a "spin" with suppressed exchange interaction between the particles. A theoretical description of the magnetic behavior of materials consisting of interacting nanoparticles has already been reported.[22] Thus, we expect to observe a difference between the magnetization of commercial Fe_2O_3 crystalline powder and the amorphous sample. In fact, Fig. 6 clearly demonstrates this effect. The coercivity field H_c and

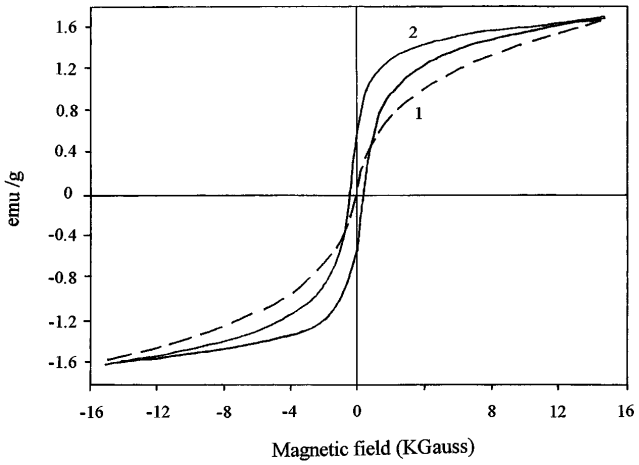

FIG. 6. Magnetization loops of (1) amorphous Fe_2O_3 and (2) commercial $\gamma-Fe_2O_3$. All the data are recorded at room temperature.

the magnetization M of amorphous Fe_2O_3 at an external field of 1.5 T are 25 G and 1.44 emu/g, respectively. For the commercial crystalline Fe_2O_3, we find $H_c = 340$ G and $M = 1.7$ emu/g. It is important to note that we could not detect a saturation of the magnetization as a function of the field or a hysteresis for the amorphous Fe_2O_3. The crystalline Fe_2O_3 shows, however, a distinctive hysteresis. This provides additional evidence that we are dealing with a superparamagnetic material. Moreover, at room temperature and a magnetic field sweep rate of 35 G/s, our sample is still above the blocking temperature; the compound is not in the spin-glass regime. For these reasons, we conclude that our sample consists of nanoparticles small enough to exhibit a superparamagnetic behavior. The magnetic behavior of amorphous Fe_2O_3 is similar to that of amorphous $Bi_3Fe_5O_{12}$, which is known to be superparamagnetic.[7] This is related to the particles' small size and their being single domain and superparamagnetic.[2]

ACKNOWLEDGMENTS

This research was supported by Grant No. 94-00230 from the US-Israel Binational Science Foundation (BSF), Jerusalem, Israel. Dr. Yu. Koltypin thanks the Ministry of Absorption, The Center for Absorption in Sciences, for its financial support. Professor A. Gedanken is grateful for the Bar-Ilan Research Authorities for supporting this project.

We thank Professor Y. Yeshurun for helpful discussions and for making the facilities of the National Center for Magnetic Measurements at the Department of Physics, Bar-Ilan University available for this study. The study of the magnetic properties was supported by the Israel Science Foundation administered by the Israeli Academy of Sciences and Humanities.

REFERENCES

1. J. Livage, J. Phys., colloque C4, supplement au no. 10, Tome 42, 981 (1981).
2. *Ferromagnetic Materials*, edited by E. P. Wohlfarth (North-Holland, Amsterdam, 1980), Vol. 2, p. 405.
3. L. Murawski, C. H. Chang, and J. D. Mackenzie, J. Non-Cryst. Solids **32**, 91 (1979).
4. H. E. Curry-Hyde, H. Musch, and A. Baiker, Appl. Catal. **65**, 211 (1990).
5. H. Cao and S. L. Suib, J. Am. Chem. Soc. **116**, 5334 (1994).
6. M. Sugimoto, J. Magn. Magn. Mater. **133**, 460 (1994).
7. K. Tanaka, K. Hirao, and N. Soga, J. Appl. Phys. **69**, 7752 (1991).
8. M. Sugimoto and N. Hiratsuka, J. Magn. Magn. Mater. **31/34**, 1533 (1983).
9. W. E. Steger, H. Landmesser, U. Boettcher, and E. Schubert, J. Mol. Struc. **217**, 341 (1990).
10. B. Pashmakov, B. Claflin, and H. Fritzsche, Solid State Commun. **86**, 619 (1993).
11. K. Kandory and T. Ishikawa, Langmuir **7**, 2213 (1991).
12. K. S. Suslick, S. B. Choe, A. A. Cichowlas, and M. W. Grinstaff, Nature (London) **353**, 414 (1991).
13. K. S. Suslick, M. Fang, T. Heyon, and A. A. Cichowlas, in *Molecularly Designed Ultrafine/Nanostructured Materials,* edited by K. E. Gonsalves, G-M. Chow, T. D. Xiao, and R. C. Cammarata (Mater. Res. Soc. Symp. Proc. **351**, Pittsburgh, PA, 1994).
14. K. S. Suslick, T. Heyon, M. Fang, and A. A. Cichowlas, *ibid.*
15. M. W. Grinstaff, M. B. Salamon, and K. S. Suslick, Phys. Rev. B **48**, 269 (1993).
16. X. Cao, Yu. Koltypin, G. Kataby, R. Prozorov, and A. Gedanken, J. Mater. Res. **10**, 2996 (1995).
17. Yu. Koltypin, X. Cao, G. Kataby, R. Prozorov, and A. Gedanken, J. Non-Cryst. Solids **201**, 159 (1996).
18. F. Feigel, *Spot Tests, Inorganic Applications* (Elsevier Publishing Co., New York, 1954), Vol. 1, pp. 154–155.
19. F. A. Cotton and G. Wilkinson, *Advanced Inorganic Chemistry* (Interscience Publishers, New York, 1962), p. 709.
20. N. N. Greenwood and T. C. Gibb, *Mössbauer Spectroscopy* (Chapman and Hall Ltd., London, 1971), p. 251.
21. S. R. Elliott, *Physics of Amorphous Materials* (Longman, London and New York, 1984), pp. 350–357.
22. S. Morup, Europhys. Lett. **28**, 671 (1994); S. Morup and E. Trone, Phys. Rev. Lett. **72**, 3278 (1994).